Food Chemistry: X 18 (2023) 100698

Contents lists available at ScienceDirect

Food Chemistry: X

journal homepage: www.sciencedirect.com/journal/food-chemistry-x

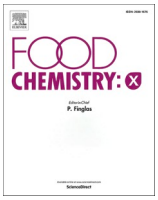

Ethanol as a switch to induce soybean lipophilic protein self-assembly and resveratrol delivery

Mingming Zhong [a,1], Yufan Sun [a,1], Hanyu Song [a], Shuai Wang [a], Baokun Qi [a,b,c], Xue Li [a,*], Yang Li [a,b,c,*]

[a] College of Food Science, Northeast Agricultural University, Harbin 150030, China
[b] National Research Center of Soybean Engineering and Technology, Harbin 150030, China
[c] Heilongjiang Green Food Science Research Institute, Harbin 150028, China

ARTICLE INFO

Keywords:
Ethanol
Soybean lipophilic protein
Resveratrol
Disassembly
Reassembly

ABSTRACT

Protein-based nanoparticles or nanocarriers of emulsion systems have piqued the interest of nutrition and health care goods. As a result, this work examines the characterisation of ethanol-induced soybean lipophilic protein (LP) self-assembly for resveratrol (Res) encapsulation, particularly the influence on emulsification. By varying the ethanol content ([E]) in the range of 0–70% (v/v), the structure, size, and morphology of LP nanoparticles may be adjusted. Similarly, the self-assembled LPs have a strong [E] dependency on the encapsulation efficiency of Res. For [E] = 40% (v/v), Res had the highest encapsulation efficiency (EE) and load capacity (LC) of 97.1% and 141.0 μg/mg nanoparticles, respectively. Most of the Res was encapsulated by the hydrophobic core of LP. Moreover, for [E] = 40% (v/v), LP-Res showed significantly improved emulsifying properties, independent of low-oil or high-oil emulsion systems. Furthermore, the ethanol-induced production of appropriate aggregates increased emulsion system stability, hence increasing Res retention during storage.

1. Introduction

Resveratrol (Res) is a natural polyphenol that can be found in the skins of various common herbs as well as grapes, apples, and peanuts. Numerous health advantages for people have been linked to it, including anti-inflammatory, anticancer, anti-platelet aggregation, cardioprotective, and anti-obesity actions (Vang et al., 2011). However, Res is vulnerable to the chemical deterioration that occurs in food, which frequently involves Res isomerization. Isomerization occurs when Res is exposed to conditions such as high temperature, extreme pH, ultraviolet (UV) light, and certain types of enzymatic hydrolysis (Davidov-Pardo & McClements, 2014). Therefore, it is particularly important to find a promising nanocarrier that is nontoxic, biodegradable, and biocompatible to improve the water solubility, stability, and bioavailability of Res.

According to the available research, soy protein has a significant deal of potential to act as a nanocarrier for drugs and nutraceuticals (Chen, Li, & Tang, 2015a; Chen, Li, & Tang, 2015b; Chen, Zhang, & Tang, 2016; Ochnio et al., 2018; Pujara, Jambhrunkar, Wong, McGuckin, & Popat, 2017). SPI is generally composed of two major storage proteins: glycinin and β-conglycinin, which account for 60–70% and 30–40% of the total protein content, respectively (Bi et al., 2018). The functional properties of SPI, such as its emulsification and solubility, depend on the interactions between these two proteins. Samoto et al. (2007) proposed a new classification system that divided SPI into three components: glycinin (23%), lipophilic protein (LP, 31%), and β-conglycinin (46%), which motivated researchers to reexamine the functional characteristics of SPI.

Oil-body membrane protein is a major LP and component of oil bodies with high affinity for oil (Sardet, Hansma, & Ostwald, 1972). Matsumura, Sirison, Ishi, & Matsumiya (2017) reported that the addition of 0.0001% LP to water decreased the surface tension of 10 mN/m; however, no changes in surface tension were observed after the addition of the same amount of glycine or β-conglobulin. Furthermore, unlike glycine and β-conglobulin, LP emulsions are stable under thermal stress and flocculation in the presence of high salt and surfactant (Tween 20) concentrations (Matsumura, Sirison, Ishi, & Matsumiya, 2017). These results indicate that the surface activity of LP is greater than those of glycine and β-conglobulin and that LP is an excellent emulsifier.

* Corresponding authors at: College of Food Science, Northeast Agricultural University, Harbin 150030, China (Y. Li).
E-mail addresses: xli_crystallee@126.com (X. Li), yangli@neau.cn (Y. Li).
[1] These authors contributed equally.

https://doi.org/10.1016/j.fochx.2023.100698
Received 8 January 2023; Received in revised form 24 April 2023; Accepted 30 April 2023
Available online 9 May 2023

Furthermore, plant proteins lack significant hydrophobic and hydrophilic partitions in their compact molecular structures and thus are rarely used to deliver hydrophobic bioactive compounds (O'Sullivan, Murray, Flynn, & Norton, 2016). Therefore, the high lipophilicity of LP can be used to deliver bioactive hydrophobic substances, which overcomes the drawbacks of common plant proteins utilized as carriers.

Previous studies have shown that the ethanol-induced soybean protein disassembly-recombination strategy can further expand the hydrophobic domain for nutrient encapsulation (Liu et al., 2019). Moreover, using ethanol as a Res solvent may eliminate interferences of other environmental factors. In addition, the amount of ethanol ([E]) used determines the extent of ethanol-induced unfolding and/or denaturation of protein structures (Tang, 2021a; Tang, 2021b). Generally, at low [E] levels, ethanol-induced protein unfolding is reversible. This indicates that when ethanol is removed (for example, by dialysis), unfolded proteins reversibly refold into their "native" protein state (Otzen, Sehgal, & Nesgaard, 2007). This process facilitates nutrient encapsulation. Peng, Xu, Li, & Tang (2020) also reported that the treatment of β-conglycinin with ethanol in the [E] range of 20–80% (v/v) significantly improved the protein emulsifying properties and interfacial stability in an [E]-dependent manner. However, the effect of LP with strong interfacial and emulsifying properties on the structure and functional characteristics of LP-Res nanoparticles after the ethanol-induced encapsulation of Res has not been examined yet.

The goal of this study is to use an ethanol-aided assembly and disassembly technique to create novel LP nanoparticles as an efficient Res nanocarrier. The reassembled LPs' size, protein denaturation, and microstructure are evaluated. Subsequently, the reassembled LP-nanoencapsulated particles are evaluated based on EE, particle size, and morphology. Finally, emulsions with different oil contents were prepared using LP–Res co-assembled nanoparticles as emulsifiers to evaluate their emulsification characteristics and stability. These findings may provide a new strategy to fabricate nonemulsifying and/or emulsifying delivery systems able to be used in food compositions and stabilized by food-grade particles.

2. Materials and methods

2.1. Materials

This study employed soybeans (Dong-Nong 42 cultivar harvested in Harbin, Heilongjiang, China, 2020) with a dry weight composition of 10.55% moisture, 40.58% crude protein, 20.47% fat, and 4.28% ash. Harbin Pu Run Fat Co., Ltd. supplied the olive oil (Harbin, Heilongjiang, China). Beijing Health Biotechnology Co., Ltd. supplied the resveratrol and ethanol (99.9%). (Beijing, China). The remaining reagents were of analytical grade. Deionized (DI) water was utilized in every experiment.

2.2. LP preparation

The isolation of LP from soybeans was performed according to a method previously reported in literature (Li et al., 2020). Briefly, defatted soybean meal (DSP) was dried at 70 °C for 2 h at a nitrogen solubility index of 75%. The dried DSP was mixed with DI water (1:8, w/v), and the pH of the resulting mixture was adjusted to 8.0 using a 2.0 M NaOH solution. The mixture was continuously stirred at 20 °C for 1 h and then centrifuged at 3000*g* (L535R-1, Xiangyi Centrifuge Co., Ltd., Hunan Changsha, China) for 10 min at 4 °C. The supernatant was separated followed by the addition of a 10 mM Na_2SO_3 aqueous solution (5 mL). The pH of the obtained mixture was adjusted to 5.8 using a 0.1 M H_2SO_4 solution. Next, the supernatant was centrifuged (3000*g*, 10 min, 4 °C), and the pH value was adjusted to 5.0 with the 0.1 M H_2SO_4 solution. The resulting system was heated to 55 °C for 15 min followed by the addition of the aqueous NaCl solution (50 mM). The pH of the produced mixture was adjusted to 5.5 with the 2.0 M NaOH solution, after which it was centrifuged at 3000*g* and 4 °C for 10 min. LP was collected and freeze-dried at −50 °C for 24 h using an FD-5 series freeze dryer (Jiangyin Xinshenbao Technology Co., Ltd., Jiangsu). The obtained sample was stored at 4 °C until further use.

2.3. Preparation of ethanol-treated reassembled LP samples

LP was dissolved in DI water overnight under magnetic stirring to obtain a stock dispersion of LP (1.0 wt%). The LP dispersion was divided into six portions and ethanol (99.9%) was added to the dispersion at an [E] of 0 (control), 10, 30, 40, 50, and 70% (v/v). After stirring these dispersions using a magnetic stirrer for 8 h, ethanol was removed by dialysis. The ethanol-treated recombinant LP samples were partially used for characterization studies (such as particle size and potential measurements), while their remaining portions were freeze-dried (Otokami Freeze Dryer Co., Ltd., China) for investigations via infrared spectroscopy and other techniques. The prepared samples were named E0, E10, E30, E40, E50, and E70, respectively.

2.4. Physical-chemical characterization of Ethanol-induced reassembled and denatured LP

Using a 4mW He-Ne laser (633 nm wavelength) at 25 °C, dynamic light scattering (DLS) investigations were carried out using a Zetasizer Nano-ZS equipment (Malvern Instruments Ltd., Malvern, Worcestershire, UK). Five analyses of each sample were performed (Sun et al., 2021).

The determination of tryptophan (Trp) in the diluted dispersions of disassembled and reassembled LP nanoparticles (protein concentration of 1.0 mg/mL in a 10 mM pH 7.0 buffer) by intrinsic emission fluorescence spectroscopy was performed using a spectrofluorometer at an excitation wavelength of 290 nm and scan speed of 1200 nm/min.

Using a DSC-204F1 thermal analyzer, differential scanning calorimetry (DSC) was used to determine the degree of protein denaturation in the various ethanol-treated samples (NETZSCH, Germany). Each protein sample (2.5 mg) was combined with 10 μL of a pH 7.0 buffer (10 mM). After equilibration was reached at room temperature (20–23 °C) for at least 5 h, the resulting mixture was sealed in an aluminum pan and subjected to DSC analysis. The thermal program was in the temperature range of 30–170 °C at a heating rate of 10 °C/min.

2.5. Ethanol-induced reassembled LP microstructure

Images created by cryo-scanning electron microscopy (Cryo-SEM) were produced using the technique described by Zhong et al. (2020). Briefly, samples were immediately frozen in liquid nitrogen at −180 °C, and then in a cryogenic preparation room, a 5 nm Pt coating was applied. The Pt-coated samples were scanned at −135 °C.

The morphology of the various ethanol-induced LP samples were investigated using a Dimension 3000 microscope (Digital Instruments-Veeco, Santa Barbara, CA, USA) and an atomic force microscope (AFM) in the tapping mode (Sun et al., 2021).

2.6. Preparation of LP-Resveratrol (LP-Res) nanoparticles

Res crystals were dissolved in 100% ethanol to create a Res stock solution (5 mg/mL). Subsequently, the prepared nanoparticle stock solution was added dropwise to a solution containing LP at a pH of 7.0 (1.0 wt%) with different [E] in the range of approximately 0–70% (v/v). In the final mixture, the ratio of LP to Res was 9:1 (w/w). Res and LP were mixed well and stirred overnight. Dialysis was used to remove the ethanol from the suspension. If necessary, the pH of the dialysis-derived suspension was adjusted to 7.0 using 0.1 M NaOH or HCl. Finally, the final LP-Res nanoparticle suspension was directly characterized or freeze-dried.

2.7. Characterization of Ethanol-induced LP-Res nanoparticles

According to a process described in the literature, the encapsulation efficiency (EE) and load capacity (LC) of Res contained in the reassembled LP particles were calculated (Zhong et al., 2022). In a nutshell, 4.5 mL of ethanol was added to 0.3 mL of the solution (c = 1.0 wt%; multiple recombinant LP samples). The result of the subsequent 60-second vortexing of the mixture was the collected supernatant (organic phase). Res in the supernatant was measured at 307 nm. According to observations of the Res standard solutions at concentrations from 0 to 24 μg/mL, a calibration curve was created. To determine the concentration of Res, the regression equation $y = 0.126x - 0.023$ ($R^2 = 0.998$) was utilized. Following are the calculations for EE and LC:

$$EE(\%) = Res\ in \frac{nanoparticles}{totalRes} \times 100 \quad (1)$$

$$LC(\%) = Res\ in \frac{nanoparticles}{totalprotein} \times 100 \quad (2)$$

A drop of the LP-Res dispersion was deposited onto a 240 mesh copper grid for TEM measurements, and 1% (w/v) phosphotungstic acid was added to the sample. An XFlash 5030 T equipment operating at 80 kV was used to take TEM images of the samples after they had dried overnight at room temperature (Sage Technology Co., Ltd., Beijing, China).

2.8. Preparation of emulsions or high internal phase emulsion (HIPE)

To evaluate the emulsifying properties of LP-Res samples treated with different [E], the emulsions and HIPE were prepared using 10% and 80% (v/v) oil content. The emulsified system was obtained using a two-step process (Zhong et al., 2020). A mixture of LP-Res dispersion and olive oil was homogenized at 10,000 rpm for 3 min using a FJ200/300-SH homogenizer (Changzhou Homogeneous Machinery Co., Ltd., Jiangsu, China) to form a coarse emulsion or HIPE. Subsequently, the resulting crude emulsion was further processed using a high-pressure homogenizer (APV2000, Shanghai Ouhe Co., Ltd., Shanghai, China) at 100 bar. The droplet size and microstructure of the produced emulsion and HIPE samples were directly characterized (Xu, Liu, & Tang, 2019).

2.9. Characterization of emulsions and HIPE

By DI water or 1% sodium dodecyl sulfate (SDS) as the dispersing solvent, the droplet size distribution curves of the various emulsions were measured using laser diffraction on a Malvern MasterSizer 2000 (Spectris Instrument Systems Co., Ltd., Shanghai, China). The ratio of the protein solution to the olive oil phase (1.455/1.34) yielded a relative refractive index of 1.096, which was used to calculate the droplet size information, including the volumetric average diameter. The total droplet interfacial area (A_t) of the protein-stabilized emulsion, which corresponds to the emulsifying properties of the protein, was directly calculated using the equation, $A_t = 6\ V_d/d_{3,2}$, where V_d is the oil volume. The flocculation state of the droplets in the fresh emulsions was evaluated using the flocculation index percentage (FI%), which was calculated according to the following Eq. (3):

$$FI(\%) = \frac{d4,3(water)}{d4,3(SDS) - 1} \times 100 \quad (3)$$

where the droplet sizes measured with water or 1% SDS as the dispersing solvent are denoted by $d_{4,3}$ (water) and $d_{4,3}$ (SDS). Assuming that each droplet's surface is covered with a dense monolayer of LP-Res molecules, the method published by Xu, Tang, Liu, and Liu (2018) was utilized to determine the surface coverage for the various ethanol-treated LP-Res samples at the interface of droplets in these HIPEs.

Proteins and lipids are labeled using confocal laser scanning microscopy (CLSM) by staining samples with Rhodamine B (protein dyeing) and Nile red (oil dyeing). To achieve excitation, light at wavelengths of 488 nm and 633 nm, respectively, is emitted by Ar/Kr and He/Ne lasers. The stained materials were divided into aliquots (10 L) and placed on concave confocal microscopy slides before being coated with coverslips. To obtain confocal images at a 100× magnification, a confocal laser scanning microscope (Woverburn Precision Machinery Co., Ltd., Suzhou, Jiangsu) equipped with an inverted microscope (Zeiss Smartproof5) was employed (Zhong et al., 2020).

2.10. Storage stability

The stability of Res encapsulation in reconstituted LP particles, emulsions, and HIPE was evaluated by determining the residual amount of Res. After 30 d of storage at 25 °C, an aliquot (100 μL) of the stored sample was removed and added to 3.0 mL of ethanol for Res extraction. The calibration curve, which was created using standard solutions in the concentration range of 0–24 μg/mL, was used to compute the concentration of Res ($y = 0.126x - 0.023$, $R^2 = 0.998$).

By directly storing the emulsions at room temperature (20–23 °C) for 30 days while measuring the thickness of the emulsions' cream and serum layers each week, the creaming index (CI) of the emulsion and HIPE samples was determined. Eq. (4) was then used to compute the CI:

$$CI(\%) = \frac{Hs}{HE} \times 100 \quad (4)$$

where Hs is the height of the clear serum layer and HE is the total height of the emulsion (or HIPE) in the tube (Keowmaneechai & McClements, 2002).

2.10. Statistical analysis

At least three different runs of each experiment were completed. The SPSS Statistics program for Windows, version 22.0, was used to analyze the data using the one-way analysis of variance (ANOVA) approach and expressed as means standard deviation (SD) (SPSS Inc., Chicago, IL, USA).

3. Results and discussion

3.1. Ethanol-induced reassembly and denaturation of LP: dependence on [E]

3.1.1. Structural reassembly of LP

The ethanol-induced reassembly phenomenon of LP proteins was characterized using DLS analysis. Table S1 contains the mean diameter (Dz) values for the particle size distribution (PSD) curves of LP (1.0 wt%) at [E] = 0–70% (v/v) and their related PSD curves, as shown in Fig. 1A. In the absence of ethanol, LP had a unimodal PSD with particle sizes in the range of 60 to 156 nm and a calculated Dz of approximately 125.0 nm. The primary PSD peaks steadily grew larger when the [E] reached 40%, and the PSD curves of the samples were bimodal at [E] = 50%. Consequently, the Dz of the particles in the dispersions steadily rose from 125.0 to 1084.3 nm as [E] increased from 0 to 70% (v/v) (Fig. 1A). These findings unequivocally demonstrate that relatively high ethanol concentrations cause LP aggregation and/or progressive protein binding. Similar results were reported for new soybean β-conglycinin (β-CG) nanoparticles made by ethanol-induced disassembly and reassembly of natural β-CG by Liu, Li, Zhang, and Tang. (2019). According to Hua et al. (2005), washing defatted soy flakes with aqueous alcohol (85%, v/v) led to a greater development of protein aggregates in the soybean protein than in the absence of the ethanol treatment.

The resultant PSD curve (Fig. 1B) shows that ethanol removal caused the PSD peaks to shift to smaller sizes and a much higher fraction of small-sized PSD peaks ([E] < 50%). Therefore, although large LP

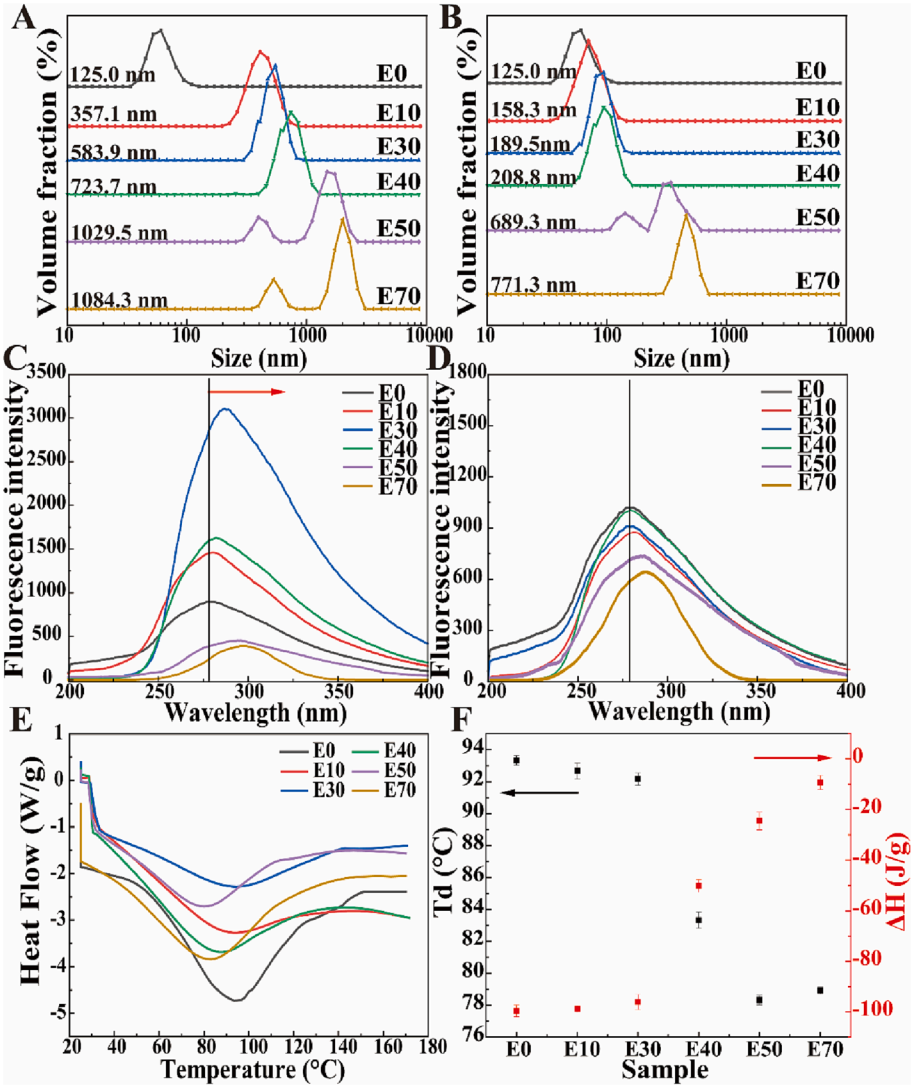

Fig. 1. Structural changes during alcohol-induced lipophilic protein (LP) disassembly and reassembly. (A) Particle size distribution of LPs during disassembly (in the presence of ethanol). (B) Particle size distribution of LPs during reassembly (after ethanol removal). (C) Disassembled LPs fluorescence spectra. (D) Fluorescence spectra of reassembled LPs. (E) DSC profiles of reassembled LPs. (F) Degree of denaturation of recombinant LPs: T_d and ΔH.

aggregates were present before ethanol removal, the structure of LP was rearranged after ethanol removal to form closely-packed LP nanoparticles, resulting in a significant reduction in particle size. Notably, the PSD curves and Dz of ethanol-treated LPs at [E] < 30% (v/v) were nearly identical to the control sample (without ethanol treatment; Fig. 1B, Table S1). This shows that the LP unfolding caused by ethanol at very low concentrations is reversible. Similar to this, Nikolaidis and Moschakis (2018) showed that whey protein isolate (WPI) denaturation caused by ethanol was minimal at [E] in the range of 10–20% (v/v).

The Tryptophan (Trp) intrinsic emission fluorescence spectra were measured at various starting [E] values in the range of 0–70% (v/v), as shown in Fig. 1C and D, to corroborate the structural rearrangement caused by LP before and after ethanol removal. The LP aggregation caused by ethanol is intimately associated with alterations in its conformation, particularly those of tertiary structures. Hydrophobic amino acid residues, such as Trp (310–325 nm), phenylalanine (Phe, 260–275 nm), and tyrosine (Tyr, 285–300 nm), that were exposed during tertiary structural changes in proteins under various conditions were detected via intrinsic fluorescence spectroscopy. The maximal wavelength (nm) of fluorescence emission from proteins' Trp chromophores increases as they are exposed to more aqueous solutions or more polar environments. When the solvent and the chromophore interact, the quenchers in the fluorophore interact with one another, lowering the quantum yield of fluorescence (Tang, Sun, & Foegeding, 2011). The impact of various [E] on the Trp intrinsic fluorescence spectra of LP is seen in Fig. 1C. The λm of the tryptophan chromophore of LP gradually increased from approximately 271 to 300 nm with gradually increasing [E] (0–70%, v/v). A similar red shift in the fluorescence of β-CG with increasing ethanol concentration was reported previously (Peng, Xu, Li, & Tang, 2020). The increased solvent accessibility of Trp residues was the explanation given by Peng & Tang. (2020) for the ethanol-assisted red shift of β-CG. Notably, the tryptophan chromophore of LP showed a stronger red shift under high [E] (70%, v/v) induction conditions (Fig. 1C). This suggests that at low [E] (<50%) levels, the red-shift phenomenon is mainly attributed to an increase in the hydrodynamic volume of protein molecules (as observed for the Dz data in Fig. 1A), with [E] > 50%, the induced structural unfolding and protein aggregation resulted in a stronger red-shift phenomena.

Furthermore, it is noteworthy that all ethanol ([E] = 0–70%)-induced LP samples were nearly identical after ethanol removal (Fig. 1D), indicating that the ethanol-induced Trp chromophore is present in LP and the change in the polarity of the microenvironment is nearly reversible. However, after ethanol removal, the fluorescence intensity of the Trp chromophore gradually increased as the initial [E]

increased from 10 to 40% (v/v), and thereafter, it decreased with increasing [E] (Fig. 1D). This shows that the LP structural unfolding and reassembly (aggregate) phenomena caused by ethanol are significantly dependent on [E] and are not entirely reversible. Whereas, ethanol removal causes structural rearrangements that develop a more compact structure, but to a limited extent. Additionally, Nikolaidis & Moschakis (2018) discovered that even when the dispersions were heavily diluted with water, denatured WPI was only partially reversible.

3.1.2. LP denaturation

DSC was used to assess the extent of ethanol-induced protein denaturation in the various reassembled LP samples. While the denaturation peak temperature (T_d) is used to evaluate protein thermal stability, enthalpy (ΔH) correlates with the proportion of undenatured protein or the degree of protein structural order (Arntfield & Murray, 1981). After ethanol removal by dialysis, the T_d and ΔH values of the reassembled LP ([E] = 10–30%, v/v) and control samples ([E] = 0%) were not significantly different (Fig. 1E and F), indicating the reversibility of intact ethanol-induced LP unfolding and refolding under lower [E] conditions. As the [E] was further increased to 70% (v/v), the thermal transition T_d and ΔH of the reassembled LP samples gradually decreased, indicating a loss of thermostability of the recombinant LP

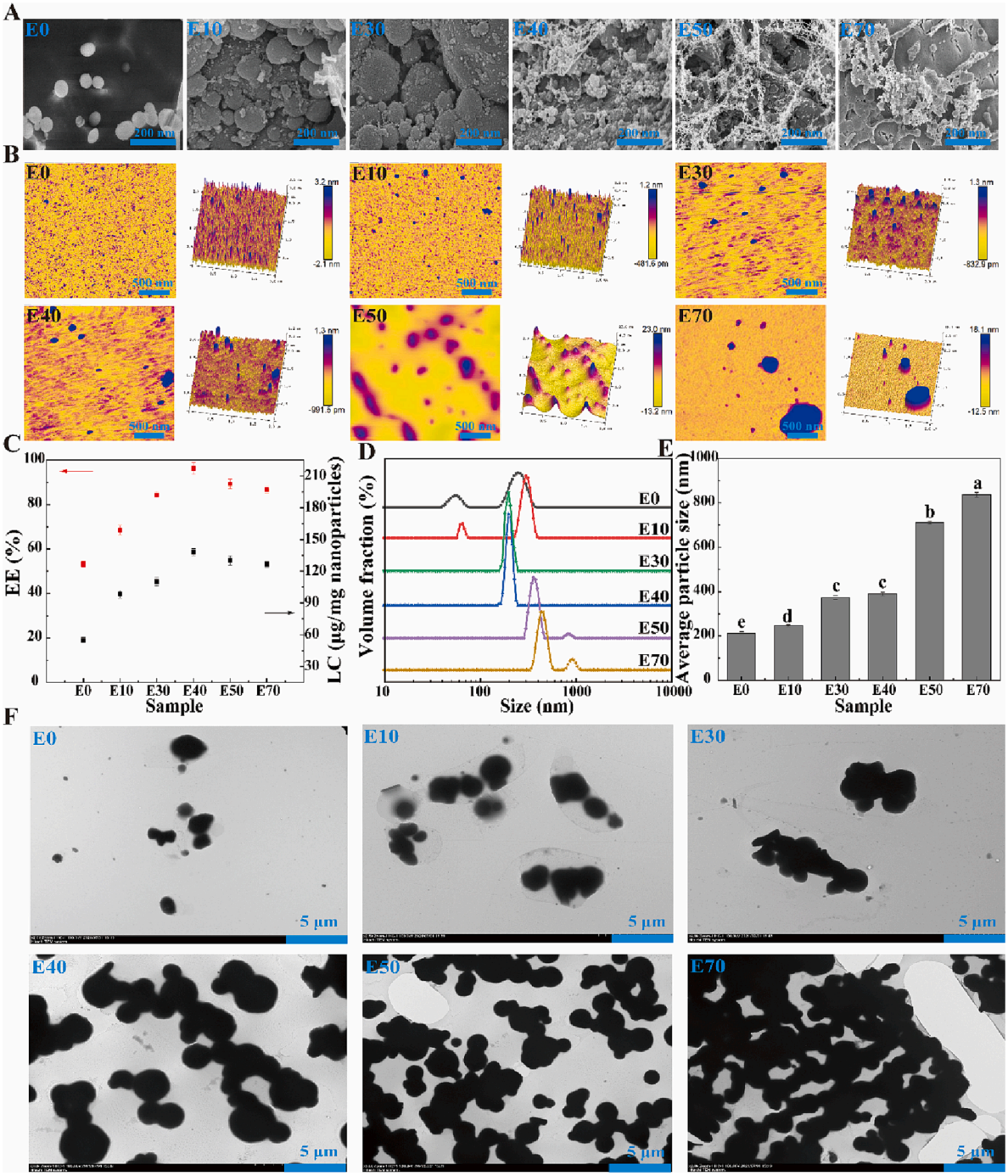

Fig. 2. Changes in microstructure after ethanol-induced LP recombination. (A) Cryo-SEM analysis. (B) AFM analysis. and characterization of nanoparticles prepared by ethanol-induced LP recombination and resveratrol (Res) encapsulation. (C) Encapsulation efficiency (EE) and loading capacity (LC). (D) Particle size distribution plot. (E) Average particle size. (F) TEM analysis.

samples, which may be caused by structural rearrangement in the denatured LP at high [E] levels by ethanol-induced unfolding, refolding, and/or reassociation of the protein. It is assumed that the proteins in LPs are in their native state at [E] = 0% (use the ΔH value at this time as an indicator of 0% denaturation), and that they then reassemble at [E] = 40–70% (v/v) in the LP samples. Notably, the percentage of LP denaturation caused by ethanol ranged from 51 to 90%. Many globular proteins, including -lactoglobulin and lysozyme, have been shown to be affected by [E] during the heat denaturation of proteins (Romero, Lozano, Sancho, & Giraldo, 2007). These results suggest that LP induction at low [E] levels (≤30%) promotes the phenomenon of reversible LP reassembly. As the [E] increases (>30%), the tertiary structure of LP changes, which induces different degrees of modification in LP, and produces a distinct aggregation phenomenon.

3.1.3. Particle microstructure

The morphology and degree of aggregation of reassembled LP samples at different initial concentrations (after ethanol removal by dialysis) at [E] = 0–70% (v/v) was analyzed using atomic force microscopy (AFM) and Cryo-scanning electron microscopy (Cryo-SEM), as shown in Fig. 2. The majority of the LP molecules existed as spherical, isolated particles with a comparatively uniform dispersion in the absence of ethanol, which is in good agreement with the DLS findings. When LP was treated with ethanol at [E] = 10–40% (v/v), the sizes of most particles in the system decreased, and small particles aggregated to form large particles with sizes of 200–400 nm (Fig. 2A and B). When [E] was further increased to 70% (v/v), it is noteworthy that most of the LP particles were highly aggregated, forming a particle-packed and inhomogeneous state with an irregular morphology and significantly increased size. In particular, at [E] = 70% (v/v), an agglomerate with a size of approximately 1.0 μm was formed. The combined DLS and DSC (Fig. 1) results clearly confirm that the degree of denaturation and aggregation of the ethanol-induced reassembled LP particles gradually increases with increasing initial [E]. Thus, the size and aggregation state of the reassembled LP particles are closely related to [E].

3.2. Characterization of LP-Res co-assembled nanoparticles

3.2.1. Encapsulation efficiency (EE) and load capacity (LC)

Considering that ethanol induces structural changes such as denaturation and aggregation of LP, the nanoencapsulation of Res in ethanol-induced LP reassembled particles were further evaluated. Initial Res and protein concentrations were 5.0 mg/mL and 1.0 wt%, respectively. After ethanol removal by dialysis, the EE and LC analyses of the reassembled LP particles with loaded Res were determined, as shown in Fig. 2C. When [E] increases from 0% to 40% (v/v), the EE and LC values increased from 52.3% and 50.2 μg/mg nanoparticles to 97.1% and 141.0 μg/mg nanoparticles, respectively. This was significantly higher than the encapsulation efficiency of ethanol induced 7S for curcumin (13.7 μg/mg, Liu et al., 2019). However, as [E] continued to increase to 70% (v/v), the EE and LC gradually decreased to approximately 88.9% and 123.6 μg/mg nanoparticles, respectively. These results indicate that the EE of Res is highly dependent on the [E] used to induce LP. At [E] = 40% (v/v), the LC and EE values reached a distinct maximum. This is because in the presence of 40% (v/v) ethanol, LP undergoes structural unfolding, accompanied by a small degree of aggregation, and when Res is introduced, the unfolded LP molecules interact with Res to form the LP-Res complex (Liu et al., 2019). Furthermore, the formation of the small amount of aggregates increases the surface area of LP in contact with Res, which may also increase the Res loading. Moreover, as ethanol ([E] = 40% (v/v)) was removed by dialysis, the LP structure exhibited a high degree of foldback recombination (as determined by the particle size and fluorescence results), and Res was encapsulated in LP during the recombination process. Thus, it is beneficial to improve the stability of Res within the molecule or between the aggregates, which is consistent with the later storage stability results.

3.2.2. Particle size and morphology of LP-Res particles

Fig. 2D shows the PSD curves of the LP-Res co-assembled nanoparticles at [E] = 0–70% (v/v), and the calculated Dz values are shown in Fig. 2E. Notably, as the [E] increased, the LP-Res nanoparticle sample gradually transformed from a bimodal PSD (containing small-size peaks, < 100 nm) to a unimodal PSD; as the [E] increased further, the PSD changed back to a bimodal curve (containing a large-size peak, approximately 1000 nm). Combined with the Dz results, the incorporation of Res was confirmed to increase the particle size of the reassembled LP-Res nanoparticles. Notably, the PSD curves were similar to those of the reconstituted LP after ethanol removal by dialysis, demonstrating that the effect of Res loading on the particle size of nanoparticles was closely dependent on structural changes (denaturation or aggregation, Fig. 1) during LP reconstitution These conclusions were further supported by TEM studies of the reassembled LP-Res particles that had been loaded with Res (Fig. 2F).

TEM observations revealed that with increasing [E], the degree of aggregation of LP-Res nanoparticles increased considerably, which was the main reason for the significant increase in the average particle size. In addition, Res-loaded reassembled LP-Res nanoparticles contained a weakly stained hydrophilic outer layer (Fig. 2F), confirming the successful Res encapsulation in LP (Zhong et al., 2022). Moreover, the LP-Res nanoparticle morphology changed significantly with increasing initial [E]. At [E] ≤ 40% (v/v), the majority of LP-Res nanoparticles exhibited regular spherical shapes, which were consistent with the Cryo-SEM data. Due to the severe aggregation phenomena, all of the particles in the Res-loaded reassembled samples had irregular shapes at [E] ≥ 50%. The difference in the particle morphology of samples prepared with different initial [E] values may be related to the differences in the ethanol-induced unfolding and aggregation rates under these varying conditions (Liu, Li, Zhang, & Tang, 2019). On the other hand, it is interesting that the ethanol-induced LP structural unfolding is inadequate to completely envelop Res if [E] is too low. Therefore, ethanol-induced unfolding can most effectively interact with Res with the hydrophobic groups of the resultant unfolded LP binding at an ideal [E] (in this study, [E] = 40%, v/v). However, excessive particle aggregation ([E] > 40%, v/v) prevents LP-Res from binding further.

3.3. Emulsification of LP-Res co-assembled nanoparticles

3.3.1. Stability of LP-Res emulsions with low oil contents

The emulsification properties of LP-Res nanoparticles were initially evaluated using emulsions with oil phase content of φ = 10% and c = 1.0 wt% and homogenization as the emulsification process. The PSD curves for LP-Res samples reconstituting using various ethanol treatments are shown in Fig. 3 for new emulsions stabilized in water or 1% SDS. The $d_{4,3}$ and $d_{3,2}$ of the droplets of these emulsions and their A_t values were calculated and listed in Table 1. Generally, the smaller the $d_{3,2}$ (in 1% SDS) of a protein-stabilized emulsion, or the larger the A_t, the better the emulsifying properties of the protein. The $d_{3,2}$ (in 1% SDS) of the stabilized emulsion of the LP-Res sample initially decreased and then increased as the [E] increased from 0 to 70%, and at [E] = 40%, the minimum value (106.8 nm) was reached. The corresponding A_t values initially increased and then decreased (Table 1), indicating that the emulsifying properties of LP-Res were improved to varying degrees in an [E]- and Res EE-dependent manner.

Using FI% and Cryo-SEM, the flocculation conditions of droplets in fresh emulsions stabilized by various [E]-induced LP-Res samples were assessed in order to identify the presence of bridging emulsion structures supporting stability. These new emulsions' FI% gradually climbed from 0.5 to 96.3% as the [E] went up from 0 to 70%. (Table 1). This shows that fresh LP-Res emulsions of ethanol-induced LP structural reorganization increase droplet flocculation in a strongly [E]-dependent way. This was further supported by Cryo-SEM or PSD curves of the emulsion (with water or 1% SDS; Fig. 3). By destroying the flocculation bridging emulsion structure, the addition of 1% SDS made guaranteed that every

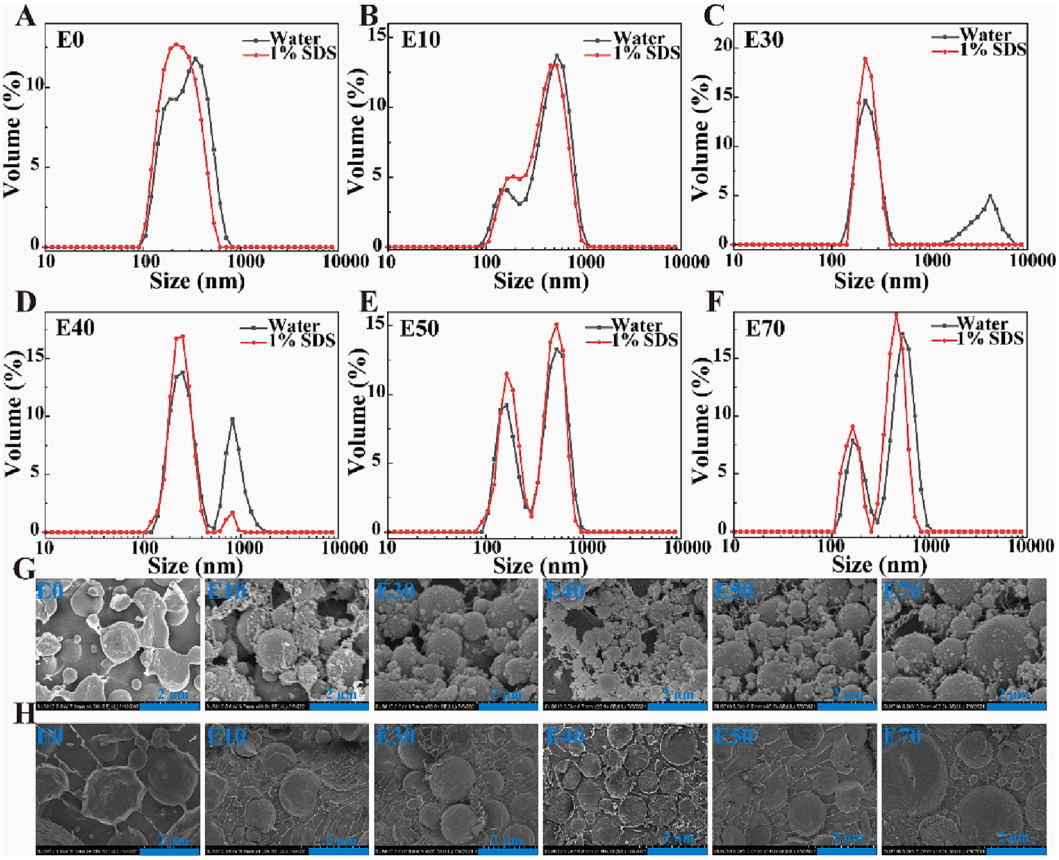

Fig. 3. Emulsification properties of LP-Res nanoparticles. (A–F) Particle size distribution curves of prepared LP-Res nanoparticle emulsions induced using different ethanol concentrations ([E] = 0–70%, v/v); and microstructural characterization of LP-Res nanoparticle-prepared emulsion and high internal phase emulsion (HIPE) systems. (G) Cryo-SEM of the emulsion system (oil phase φ = 10%). (H) Cryo-SEM of the HIPE system (φ = 80%).

Table 1
Volumetric- or surface-average droplet size ($d_{4,3}$ or $d_{3,2}$; obtained using water or 1% SDS as the dispersing solvent), total interfacial area (A_t), and flocculation index (FI) of fresh emulsions stabilized by ethanol treatment at different concentrations of [E] = 0–70% (v/v).*

Sample	Droplet Size (nm) $d_{4,3}$		$d_{3,2}$		A_t (m^2/g)	FI (%)
	water	1 %SDS	water	1 %SDS		
E0	568.3 ± 1.3^{f}	493.4 ± 2.5^{d}	263.5 ± 6.8^{a}	231.3 ± 2.6^{a}	635.3 ± 32.6^{f}	0.5 ± 0.1^{f}
E10	652.6 ± 2.7^{e}	621.6 ± 4.2^{a}	257.3 ± 1.5^{a}	217.3 ± 3.1^{b}	754.6 ± 21.4^{e}	5.2 ± 0.6^{e}
E30	666.2 ± 5.3^{d}	582.3 ± 3.6^{b}	241.6 ± 6.2^{b}	201.7 ± 3.3^{c}	1074.4 ± 9.6^{d}	16.3 ± 0.8^{d}
E40	734.5 ± 6.4^{c}	553.4 ± 5.6^{c}	226.3 ± 2.7^{c}	106.8 ± 1.9^{f}	1684.7 ± 10.1^{a}	49.2 ± 1.6^{c}
E50	852.4 ± 8.2^{b}	549.3 ± 9.4^{c}	174.3 ± 4.2^{d}	139.5 ± 5.0^{e}	1274.2 ± 31.1^{c}	88.6 ± 2.3^{b}
E70	962.8 ± 7.3^{a}	546.2 ± 7.1^{c}	148.5 ± 2.5^{e}	185.3 ± 1.3^{d}	1371.0 ± 23.5^{b}	96.3 ± 1.1^{a}

*Values with different superscripts in the same column are significantly different at $p < 0.05$. E0–E70 represents [E] = 0–70% v/v.

droplet was in an isolated state. In the absence of 1% SDS, as shown in Fig. 3, two PSD groups (denoted as I and II) of droplets were observed for the fresh emulsions with peak sizes of approximately 300 nm and 1 μm, respectively. With increasing [E] (>40%), the size distribution peak gradually shifted to the right in the LP-Res stabilized emulsion. The droplet distribution drastically altered to smaller particle sizes in the presence of 1% SDS. This indicates that [E] > 40% clearly causes flocculation and aggregation of droplets. Considering that the particle size of ethanol-treated LPs with [E] > 40% is much larger than those with [E] ≤ 40% (Fig. 1A and B), it is reasonable to assume that the proper aggregation of LP induced by ethanol ([E] = 40%, FI = 49.2%) enhances the emulsifying properties and further promotes the formation of flocculated microstructures in the emulsion. Conversely, excessive aggregation ([E] > 40%) reduces the emulsifying performance and stability. Therefore, when [E] grew, the flocculation state of the droplets in the fresh emulsions steadily increased. This was further supported by Cryo-SEM (Fig. 3G and H).

3.3.2. Stability of the LP-Res high internal phase emulsion (HIPE)

The effects of ethanol treatment on the emulsifying properties and interfacial coverage of LP-Res at different [E] levels were also evaluated using a HIPE system at φ = 80% and c = 1.0 wt%. All the HIPEs obtained from LP-Res samples treated with different [E] levels were stable and homogeneous with poor flow behavior, whereas LPs without ethanol treatment did not form stable HIPEs. From the state of the HIPE in the inverted vial, it is noteworthy that all the HIPEs exhibited a self-supporting gel network with the exception of the LP samples that were not treated with ethanol and those treated with 10% ethanol (Fig. 4B). Combined with Cryo-SEM and CLSM, it is demonstrated that the formation of the HIPE gel network mainly occurs via the droplet bridging mechanism. In HIPE gels stabilized with suitable quantities of ovalbumin and β-CG, similar effects were also seen (Xu, Tang, Liu, & Liu, 2018; Xu, Liu, & Tang, 2019).

The droplet $d_{3,2}$ of the fresh HIPEs and the surface coverage at the interface were determined as a function of [E], as listed in Table S2. As expected, the $d_{3,2}$ of the HIPEs initially decreased and then increased with increasing [E] from 0 to 70% (v/v), confirming that ethanol

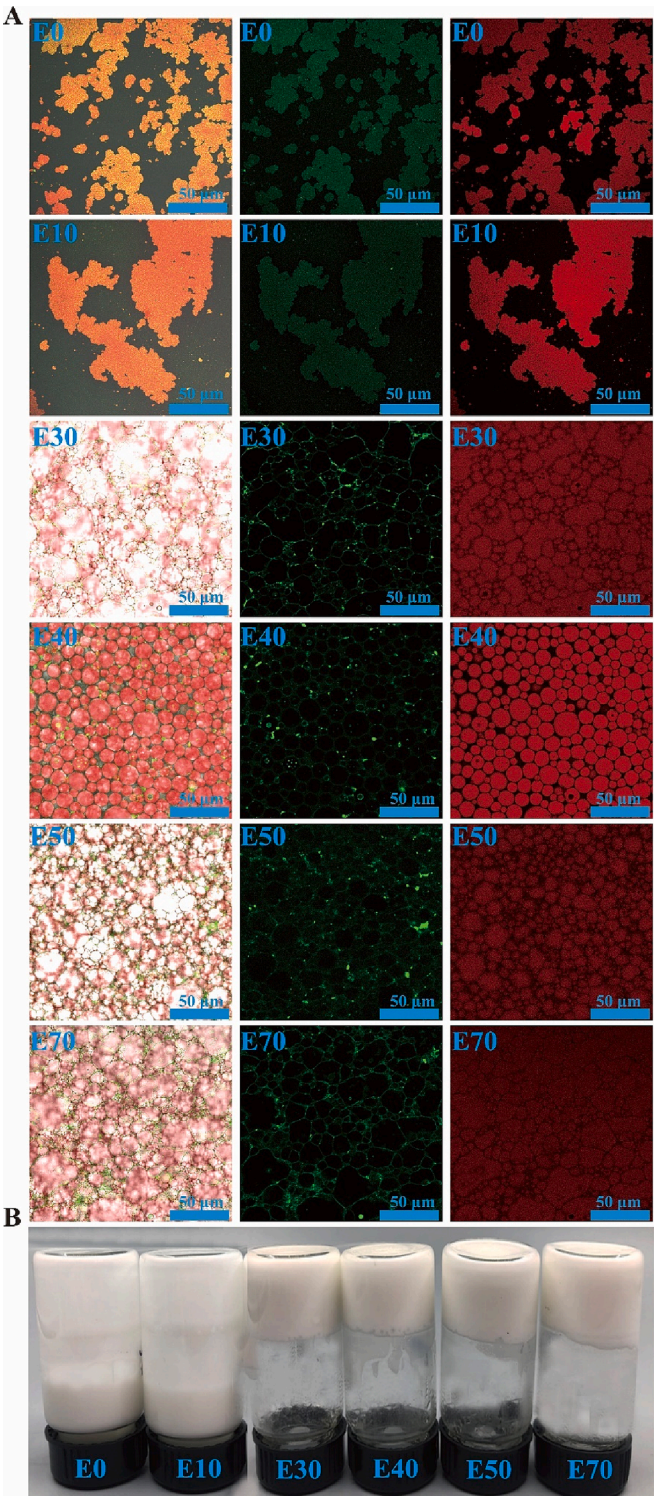

Fig. 4. (A) CLSM and (B) raw images of LP-Res nanoparticles prepared using the HIPE system.

treatment of LPs significantly improves its emulsifying properties, even in the HIPE system. The coverage of untreated LP-stabilized HIPE (~85%) was similar to that of β-CG-stabilized HIPE (~83%; Peng, Xu, Li, & Tang, 2020). Notably, when LP was treated with ethanol to encapsulate Res, the coverage of HIPE was significantly reduced (Table S2). For example, the coverage of ethanol-treated LP-Res for stable HIPE at [E] = 40% was 1.3%, which is lower than that reported for ethanol-induced β-CG nanoparticles (1.5–2.8%) (Peng, Xu, Li, & Tang, 2020), in which the fabricated nanoparticles functioned as excellent Pickering stabilizers. Therefore, these results indicate that ethanol treatment of LP-Res further enhances the interfacial filling efficiency of nanoparticles when used to stabilize HIPE, in addition to improving the emulsifying properties, which is consistent with the CLSM results.

3.4. Stability of Res in LP-Res nanoparticles, emulsion and HIPE

The oil precipitation rate and Res retention were measured to evaluate the stability of LP-Res nanoparticles prepared from ethanol-treated LP, emulsion (low-oil content) and HIPE (high-oil content) systems and Res encapsulation after 30 d of long-term storage (Fig. 5A). With a gradual increase in [E], the Res retention initially increased and then decreased, independent of whether it was in the LP-Res nanoparticles, emulsion or HIPE system. It is recognized that Res is easily degraded during storage (Liu, Fan, Gao, Zhang, & Yi, 2018). With increasing [E], the Res retention in the nanoparticles significantly improved compared with the natural LP-encapsulated Res. At [E] = 40%, the Res retention of the recombinant LP-Res nanoparticles was 84.23% after storage for 30 d. This indicates that ethanol induces LP unfolding and the recombination process to encapsulate Res in LP molecules or between aggregate particles significantly improves the stability of nanoparticles during storage. Khan, Chen, & Liang (2021) used hollow zein to encapsulate Res and chitosan coating to improve nanoparticle stability, and found that the storage retention of Res was 78%. Other studies have shown that protein or polysaccharide-enhanced protection have enhanced shielding effects for environmental factors, such as pH, temperature, etc., and impedes the release of Res (Chen et al., 2020).

Fig. 5B shows the Res retention and oil leaching of the low-oil emulsions stored for 30 d. In the absence of ethanol induction, the Res retention in LP-Res decreased to below 20% of its initial encapsulation value, and the oil precipitation rate was 78.4%. This indicates that the interfacial protection of LP-Res on the emulsion was significantly reduced ($p < 0.05$). When ethanol induces LP to reconstitute and encapsulate Res to form an emulsion prepared by nanoparticles, the oil precipitation rate was significantly reduced, and the Res retention increased. In particular, at [E] = 40%, the oil precipitation rate was 14.3% and the Res retention was 79.6%. The previous particle size and A_t results indicate that ethanol-induced LP aggregation enhances its emulsifying properties, thereby further promoting the formation of bridging emulsion structures, which are favorable for improving the stability. The formation of appropriate aggregates and bridging dairy structures were reported to favor the formation of more stable emulsified interfacial structures for LP-Res nanoparticles (Gharsallaoui et al., 2010). Thus, the emulsion stability decreased at [E] > 40%. As expected, LP-Res nanoparticle-stabilized HIPE and emulsion systems exhibited similar behavior, with the highest Res retention and the lowest oil leaching observed at [E] = 40% (Fig. 5C). Interestingly, the HIPE system protected Res more effectively than the nanoparticles and emulsion. At [E] = 40%, the Res retention rate was 87.36%. The structural unfolding and rearranging of the particles at the contact, which encourages the creation of the gel network, is assumed to be the cause of the heightened lateral attractive interactions between the particles at the interface. The results for HIPEs or HIPE gels stabilized by many globular proteins have been similar (Sun et al., 2022, Du et al., 2022). These results suggest that LP structural reorganization induced at an appropriate [E] serves as an excellent Res carrier. Moreover, the Res loading further improves the emulsification and stability of LP-Res nanoparticles. This property is essential for the application of these nanoparticles, emulsions and HIPEs in food formulations that require high storage stability.

4. Conclusions

In this study, ethanol-induced LP nanoparticles were used to encapsulate Res for the first time and prepare emulsions (10% oil content, w/w) and HIPEs (80% oil content, w/w) with high emulsification

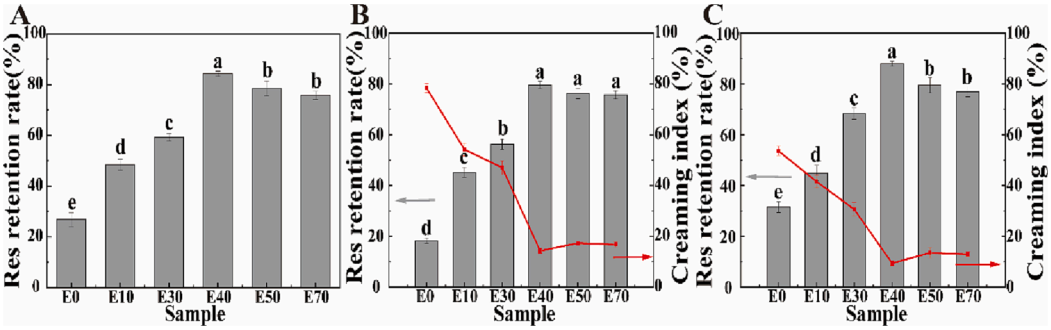

Fig. 5. Emulsion system and Res stability characterization. (A) Res retention of LP-Res nanoparticles after 30 d of storage. (B) Res retention and cream index (CI) of LP-Res emulsions stored after 30 d of storage. (C) Res retention and CI in the HIPE system prepared from LP-Res after 30 d of storage.

degrees and stability. By adjusting [E] to caused LP self-assembly in the range of 0–70% (v/v), one may changed the size and shape of LP and LP-Res particles. Before ethanol removal by dialysis, the degree of LP aggregation and denaturation gradually increased with increasing [E]. After reconstitution, LP particles with [E] = 40% exhibited the highest Res loading capacity with an EE and LC of 97.1% and 141.0 μg/mg nanoparticles, respectively. At [E] = 40% (v/v), the reassembled particles' ideal encapsulation performance is roughly linked to the ethanol-induced reversible reassembly of LP molecules and the formation of appropriate aggregates, which favors the complete interaction of unfolded LPs with Res. The reassembled LP-Res nanoparticles can be used as excellent emulsifiers to prepare emulsions and HIPEs, thereby significantly improving the stability of Res. The development of food-grade protein nanoparticles and emulsification techniques as efficient nanocarriers to increase the EE and stability of poorly soluble bioactive compounds is significantly affected by these findings. The findings of this study can facilitate the preparation of various types of food with desired functional characteristics by utilizing different carrier forms of natural edible biopolymers.

Author statement

M.Z. conceived and designed the experiments, conducted the experiments, wrote the manuscript, provided funding; Y.S., H.S., and S.W. conducted the experiments; Y.L. supervised; B.Q. reviewed and edited the manuscript, provided funding.

Declaration of Competing Interest

The authors declare that they have no known competing financial interests or personal relationships that could have appeared to influence the work reported in this paper.

Data availability

Data will be made available on request.

Acknowledgements

The authors gratefully acknowledge the financial support received from the China Scholarship Council (No. 202106610013) and National Natural Science Foundation of China (Grant no. 32172141).

Appendix A. Supplementary data

Supplementary data to this article can be found online at https://doi.org/10.1016/j.fochx.2023.100698.

References

Arntfield, S. D., & Murray, E. D. (1981). The influence of processing parameters on food protein functionality I. Differential scanning calorimetry as an indicator of protein denaturation. *Canadian Institute of Food Science and Technology Journal, 14*(4), 289–294.

Bi, C. H., Zhu, Y. D., Li, L. T., Zhang, Y. L., Hua, Z., Zhu, J. Y., … Huang, Z. G. (2018). Rheological properties and microstructure of soy protein isolate/κ-carrageenan gels under high-speed shear treatment. *Journal of Food Engineering, 236*, 44–50.

Chen, F. P., Li, B. S., & Tang, C. H. (2015a). Nanocomplexation between curcumin and soy protein isolate: Influence on curcumin stability/bioaccessibility and in vitro protein digestibility. *Journal of Agricultural and Food Chemistry, 63*(13), 3559–3569.

Chen, F. P., Li, B. S., & Tang, C. H. (2015b). Nanocomplexation of soy protein isolate with curcumin: Influence of ultrasonic treatment. *Food Research International, 75*, 157–165.

Chen, F. P., Zhang, N., & Tang, C. H. (2016). Food proteins as vehicles for enhanced water dispersibility, stability and bioaccessibility of coenzyme Q10. *LWT-Food Science and Technology, 72*, 125–133.

Chen, S., Ma, X., Han, Y., Wei, Y., Guo, Q., Yang, S., … Gao, Y. (2020). Effect of chitosan molecular weight on zein-chitosan nanocomplexes: Formation, characterization, and the delivery of quercetagetin. *International Journal of Biological Macromolecules, 164*, 2215–2223.

Davidov-Pardo, G., & McClements, D. J. (2014). Resveratrol encapsulation: Designing delivery systems to overcome solubility, stability and bioavailability issues. *Trends in Food Science & Technology, 38*(2), 88–103.

Du, X., Hu, M., Liu, G., Qi, B., Zhou, S., Lu, K., … Li, Y. (2022). Development and evaluation of delivery systems for quercetin: A comparative study between coarse emulsion, nano-emulsion, high internal phase emulsion, and emulsion gel. *Journal of Food Engineering, 314*, Article 110784.

Gharsallaoui, A., Saurel, R., Chambin, O., Cases, E., Voilley, A., & Cayot, P. (2010). Utilisation of pectin coating to enhance spray-dry stability of pea protein-stabilised oil-in-water emulsions. *Food Chemistry, 122*(2), 447–454.

Hua, Y., Huang, Y., Qiu, A., & Liu, X. (2005). Properties of soy protein isolate prepared from aqueous alcohol washed soy flakes. *Food Research International, 38*(3), 273–279.

Keowmaneechai, E., & McClements, D. J. (2002). Influence of EDTA and citrate on physicochemical properties of whey protein-stabilized oil-in-water emulsions containing $CaCl_2$. *Journal of Agricultural and Food Chemistry, 50*(24), 7145–7153.

Khan, M. A., Chen, L., & Liang, L. (2021). Improvement in storage stability and resveratrol retention by fabrication of hollow zein-chitosan composite particles. *Food Hydrocolloids, 113*, Article 106477.

Li, Y., Zhong, M., Xie, F., Sun, Y., Zhang, S., & Qi, B. (2020). The effect of pH on the stabilization and digestive characteristics of soybean lipophilic protein oil-in-water emulsions with hypromellose. *Food Chemistry, 309*, Article 125579.

Liu, L. L., Li, X. T., Zhang, N., & Tang, C. H. (2019). Novel soy β-conglycinin nanoparticles by ethanol-assisted disassembly and reassembly: Outstanding nanocarriers for hydrophobic nutraceuticals. *Food Hydrocolloids, 91*, 246–255.

Liu, Y., Fan, Y., Gao, L., Zhang, Y., & Yi, J. (2018). Enhanced pH and thermal stability, solubility and antioxidant activity of resveratrol by nanocomplexation with α-lactalbumin. *Food & Function, 9*(9), 4781–4790.

Matsumura, Y., Sirison, J., Ishi, T., & Matsumiya, K. (2017). Soybean lipophilic proteins – Origin and functional properties as affected by interaction with storage proteins. *Current Opinion in Colloid & Interface Science, 28*, 120–128.

Nikolaidis, A., & Moschakis, T. (2018). On the reversibility of ethanol-induced whey protein denaturation. *Food Hydrocolloids, 84*, 389–395.

Ochnio, M. E., Martínez, J. H., Allievi, M. C., Palavecino, M., Martínez, K. D., & Pérez, O. E. (2018). Proteins as nano-carriers for bioactive compounds. The case of 7S and 11S soy globulins and folic acid complexation. *Polymers, 10*(2), 149.

O'sullivan, J., Murray, B., Flynn, C., & Norton, I. (2016). The effect of ultrasound treatment on the structural, physical and emulsifying properties of animal and vegetable proteins. *Food Hydrocolloids, 53*, 141–154.

Otzen, D. E., Sehgal, P., & Nesgaard, L. W. (2007). Alternative membrane protein conformations in alcohols. *Biochemistry, 46*(14), 4348–4359.

Peng, L. P., & Tang, C. H. (2020). Outstanding antioxidant pickering high internal phase emulsions by co-assembled polyphenol-soy β-conglycinin nanoparticles. *Food Research International, 136*, Article 109509.

Peng, L. P., Xu, Y. T., Li, X. T., & Tang, C. H. (2020). Improving the emulsification of soy β-conglycinin by alcohol-induced aggregation. *Food Hydrocolloids, 98*, Article 105307.

Pujara, N., Jambhrunkar, S., Wong, K. Y., McGuckin, M., & Popat, A. (2017). Enhanced colloidal stability, solubility and rapid dissolution of resveratrol by nanocomplexation with soy protein isolate. *Journal of Colloid and Interface Science, 488*, 303–308.

Romero, C. M., Lozano, J. M., Sancho, J., & Giraldo, G. I. (2007). Thermal stability of β-lactoglobulin in the presence of aqueous solution of alcohols and polyols. *International Journal of Biological Macromolecules, 40*(5), 423–428.

Samoto, M., Maebuchi, M., Miyazaki, C., Kugitani, H., Kohno, M., Hirotsuka, M., & Kito, M. (2007). Abundant proteins associated with lecithin in soy protein isolate. *Food Chemistry, 102*, 317–322.

Sardet, C., Hansma, H., & Ostwald, R. (1972). Characterization of guinea pig plasma lipoproteins: The appearance of new lipoproteins in response to dietary cholesterol. *Journal of Lipid Research, 13*, 624–639.

Sun, Y., Zhang, S., Xie, F., Zhong, M., Jiang, L., Qi, B., & Li, Y. (2021). Effects of covalent modification with epigallocatechin-3-gallate on oleosin structure and ability to stabilize artificial oil body emulsions. *Food Chemistry, 341*, Article 128272.

Sun, Y., Zhong, M., Sun, Y., Li, Y., Qi, B., & Jiang, L. (2022). Stability and digestibility of encapsulated lycopene in different emulsion systems stabilized by acid-modified soybean lipophilic protein. *Journal of the Science of Food and Agriculture, 102*(13), 6146–6155.

Tang, C. H. (2021a). Assembly of food proteins for nano-encapsulation and delivery of nutraceuticals (a mini-review). *Food Hydrocolloids, 117*, Article 106710.

Tang, C. H. (2021b). Nano-architectural assembly of soy proteins: A promising strategy to fabricate nutraceutical nanovehicles. *Advances in Colloid and Interface Science, 291*, Article 102402.

Tang, C. H., Sun, X., & Foegeding, E. A. (2011). Modulation of physicochemical and conformational properties of kidney bean vicilin (phaseolin) by glycation with glucose: Implications for structure–function relationships of legume vicilins. *Journal of Agricultural and Food Chemistry, 59*(18), 10114–10123.

Vang, O., Ahmad, N., Baile, C. A., Baur, J. A., Brown, K., Csiszar, A., … Ma, Q. Y. (2011). What is new for an old molecule? Systematic review and recommendations on the use of resveratrol. *PloS One, 6*(6), Article e19881.

Xu, Y. T., Liu, T. X., & Tang, C. H. (2019). Novel pickering high internal phase emulsion gels stabilized solely by soy β-conglycinin. *Food Hydrocolloids, 88*, 21–30.

Xu, Y. T., Tang, C. H., Liu, T. X., & Liu, R. (2018). Ovalbumin as an outstanding Pickering nanostabilizer for high internal phase emulsions. *Journal of Agricultural and Food Chemistry, 66*(33), 8795–8804.

Zhong, M., Sun, Y., Sun, Y., Wang, Q., Qi, B., & Li, Y. (2022). Determination of the pH- and thermal stability mechanism of lipophilic protein-hydroxypropyl methylcellulose oil-in-water emulsion. *LWT, 155*, Article 112969.

Zhong, M., Xie, F., Zhang, S., Sun, Y., Qi, B., & Li, Y. (2020). Preparation and digestive characteristics of a novel soybean lipophilic protein-hydroxypropyl methylcellulose-calcium chloride thermosensitive emulsion gel. *Food Hydrocolloids, 106*, Article 105891.